Supporting Information:

The effect of solvent on convectively-driven silica particle assembly: Decoupling surface tension, viscosity, and evaporation rate

Lucien Roach[1], David Gonzalez-Rodriguez[2], Jie Gao[3], Eric Laurichesse[4],*

Alexander Castro-Grijalba[1], Reiko Oda[3], Véronique Schmitt[4], Emilie Pouget[3]

Mona Tréguer-Delapierre[1], Glenna L. Drisko[1]*

[1] Université de Bordeaux, CNRS, Bordeaux INP, ICMCB, UMR 5026, F-33600 Pessac, France.

lucien.roach@icmcb.cnrs.fr; glenna.drisko@icmcb.cnrs.fr

[2] Université de Lorraine, LCP-A2MC, 57000 Metz, France.

[3] Université de Bordeaux, CNRS, Bordeaux INP, CBMN, UMR 5248, F-33600 Pessac, France.

[4] Université de Bordeaux, CNRS, CRPP, UMR 5031, 33600 Pessac, France.

Section S1. Physical properties of methanol, ethanol, isopropanol and t-butanol

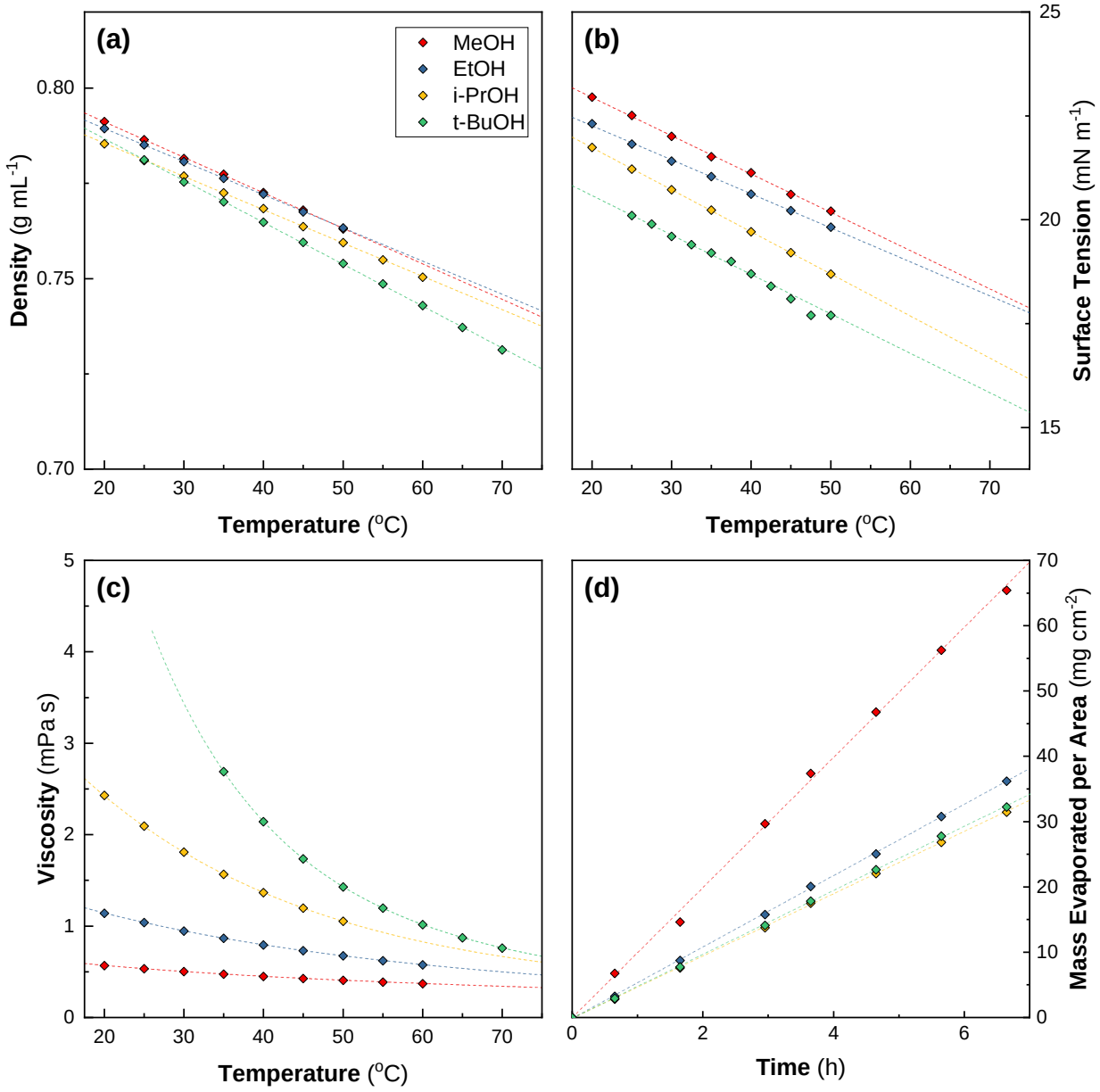

Figure S1. (a) Experimental densities of alcohols used in this study as a function of temperature as taken from the literature.[1–4] The lines are linear fits. (b) Experimental surface tensions of alcohols used in this study as a function of temperature, taken from literature.[5,6] The lines are linear fits. (c) Experimental dynamic viscosities of alcohols used in this study as a function of temperature, taken from literature.[2,7,8] The lines are an exponential decay function fitted to the data. (d) Evaporative fluxes of MeOH, EtOH, i-PrOH, and t-BuOH at 50 °C. Evaporative fluxes were 33 mg h^{-1} cm^{-2} for MeOH, 18 mg h^{-1} cm^{-2} for EtOH, 16 mg h^{-1} cm^{-2} for i-PrOH, and 16 mg h^{-1} cm^{-2} for t-BuOH. The lines are linear fits.

Section S2. SiO_2 seed particles (30 nm)

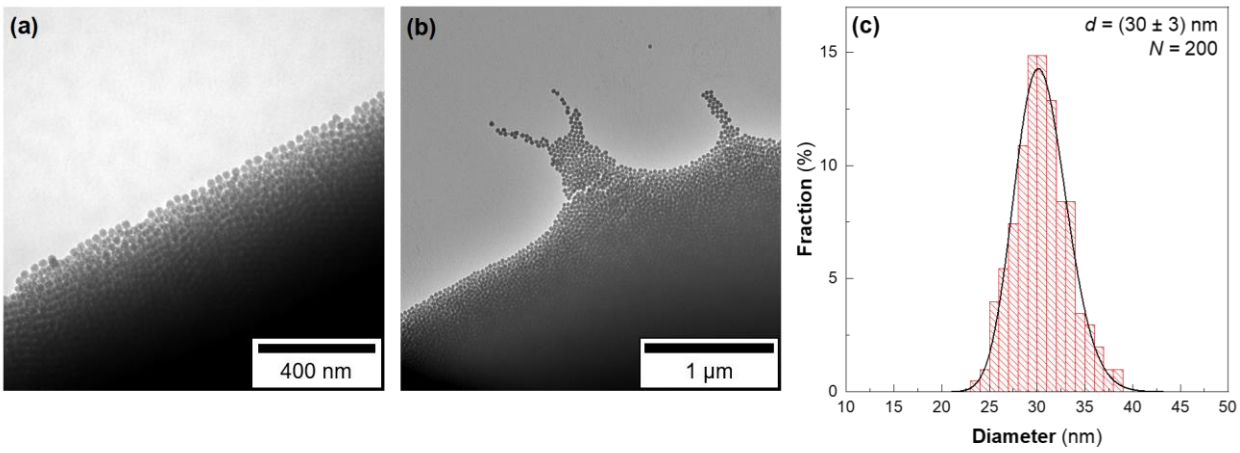

Figure S2. (a & b) TEM micrographs of as-prepared SiO_2 seed particles (30 nm) used in this study. (c) Measured size distribution of the SiO_2 seed particles. Diameter, d, is given as ($d \pm \sigma_d$) nm.

Section S3. Synthesis of SiO_2 particles (250 nm)

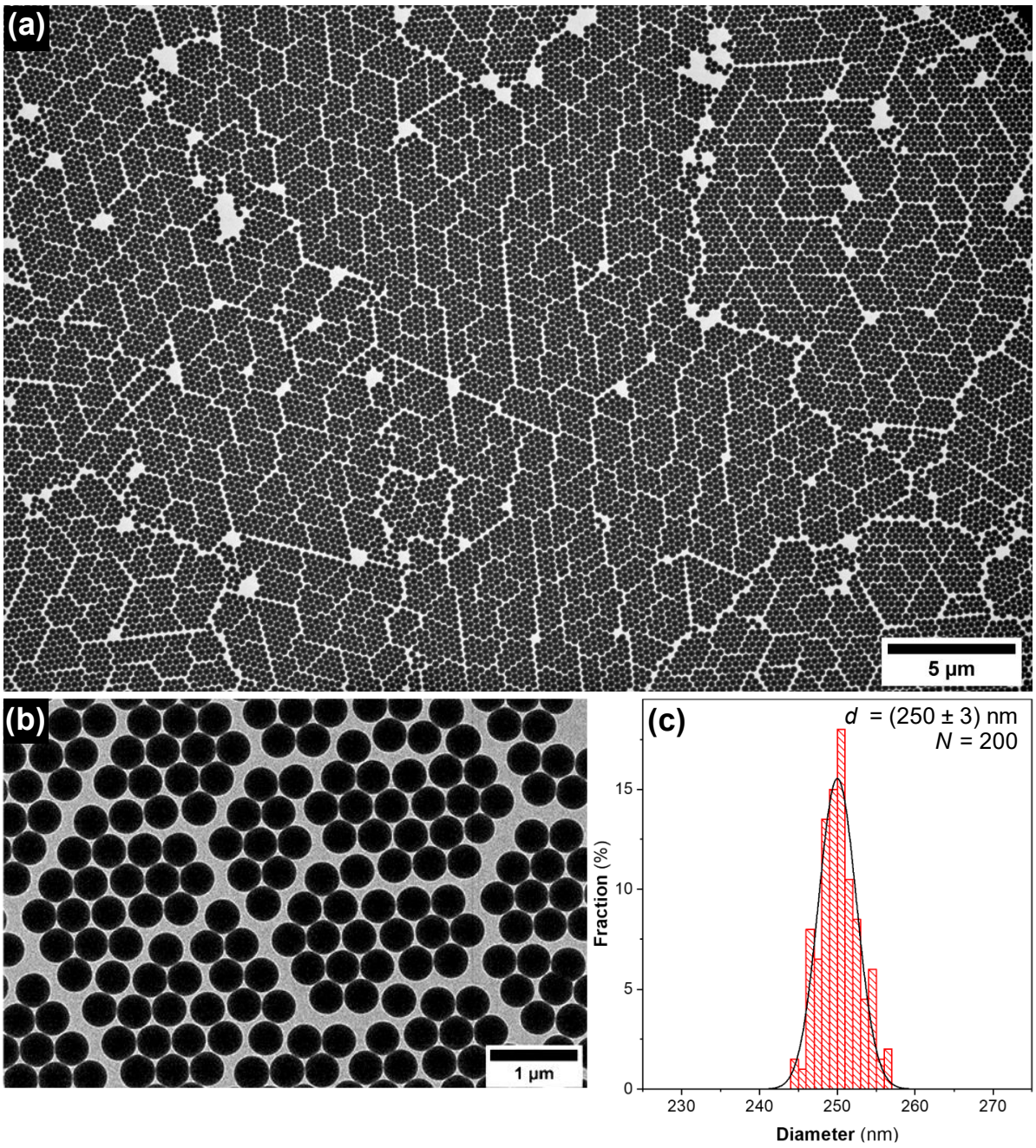

Figure S3. (a) Low magnification TEM micrograph (600×) of as-prepared SiO_2 particles (250 nm) used in this study. (b) Higher magnification TEM micrograph (6000×) of the same as-prepared SiO_2 particles. (c) Measured size distribution of the SiO_2 particles.

Section S4. Films drawn from alcohols with varying viscosity and withdrawal rate

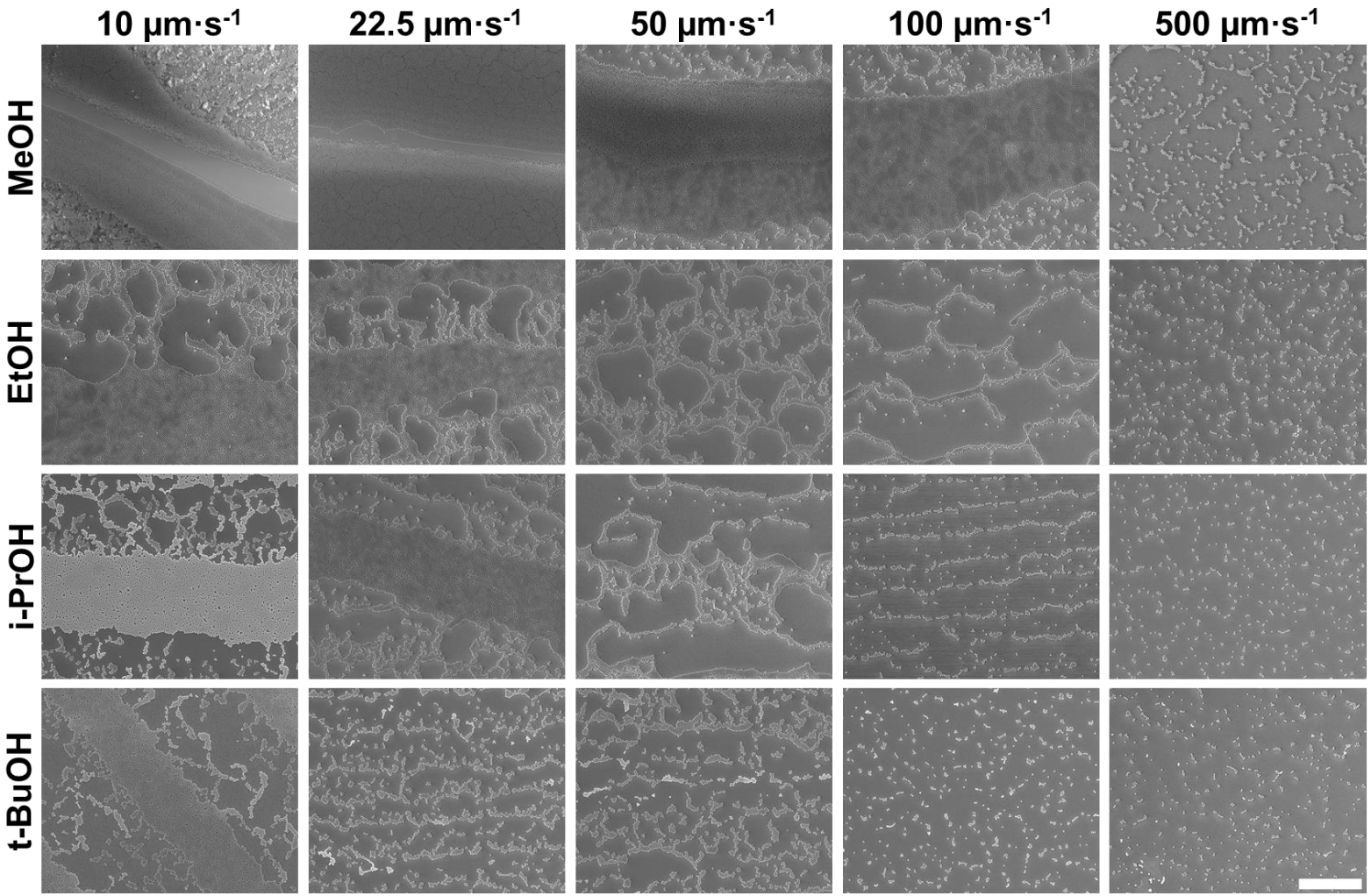

Figure S4. Colloidal films prepared *via* dip-coating in different solvents at different withdrawal rates using 0.1 vol% 250 nm SiO_2 particles with a chamber temperature of 50 °C. All images were taken at the same magnification. The scale is the same for all images, the scale bar represents 10 μm.

Section S5. Normalizing withdrawal velocity for evaporative effects

The surface coverage of a dip-coated film can be approximated by:[9]

$$S = c_1 L_c Ca^{\frac{2}{3}} + c_2 L_c \frac{V_e}{V} \tag{S1}$$

Where S is the surface coverage, c_1 and c_2 are constants, L_c is the capillary length, Ca is the capillary number, V_e is the evaporative flux, and V is the withdrawal velocity. In the convective regime $c_1 L_c Ca^{2/3} \ll c_2 L_c \frac{V_e}{V}$, hence the contributions of the first term can be ignored, and the expression rearranged to:

$$\frac{S}{L_c V_e} = \frac{c_2}{V} \tag{S2}$$

Which is constant for a fixed withdrawal velocity, hence for two solvents S_1 and S_2:

$$\frac{S^{(S_1)}}{L_c^{(S_1)} V_e^{(S_1)}} = \frac{S^{(S_2)}}{L_c^{(S_2)} V_e^{(S_2)}} \tag{S3}$$

If EtOH is selected as a reference solvent (S_2), this can be rearranged to:

$$S^* = S \frac{L_c^{(\mathrm{EtOH})} V_e^{(\mathrm{EtOH})}}{L_c V_e} \tag{S4}$$

Which gives the expected surface coverage when rescaled by the capillary length and evaporation rate of ethanol. Ethanol was arbitrarily chosen as the reference solvent, which changes the absolute magnitude, but not the relative magnitude of the rescaled surface coverage values. Any difference in the relative magnitudes of the surface coverage before and after rescaling would thus suggest that evaporative effects are responsible for the observed changes in surface coverage. We can insert this value into eq. S2 to derive a normalized withdrawal velocity, $V^* = V \frac{L_c V_e}{L_c^{(\mathrm{EtOH})} V_e^{(\mathrm{EtOH})}}$, which is rescaled to account for differences in evaporation rate.

$$S^* = \frac{L_c^{(\mathrm{EtOH})} V_e^{(\mathrm{EtOH})}}{L_c V_e} \frac{c_2 L_c V_e}{V} = \frac{c_2 L_c V_e}{V^*} \tag{S5}$$

Section S6. Isopropanol/glycerol/silica composition evolution during evaporation

Table S1. Composition of solutions used in the rheology measurements shown in Figures 3a, S5, and S6. All concentrations are expressed as volume fractions. Equivalent solutions contain the same ratio of glycerol to isopropanol as the isopropanol – glycerol – SiO_2 particle solutions to the right.

Isopropanol – Glycerol – SiO_2 solutions				Equivalent Isopropanol – Glycerol solutions	
Glycerol ϕ_{glyc}	**SiO_2** ϕ_{SiO2}	**Isopropanol** ϕ_{IPA}		**Glycerol** ϕ_{glyc}	**Isopropanol** ϕ_{IPA}
- -	- -	- -		0	1
0.005	0.0011	0.994	→	0.005	0.995
0.015	0.0033	0.982	→	0.015	0.985
0.05	0.011	0.939	→	0.053	0.947
0.1	0.022	0.878	→	0.102	0.898
0.15	0.033	0.817	→	0.159	0.841
0.2	0.044	0.756	→	0.209	0.791
0.25	0.055	0.695	→	0.269	0.731
0.3	0.066	0.634	→	0.321	0.679
0.4	0.088	0.512	→	0.434	0.566
- -	- -	- -		0.562	0.438
- -	- -	- -		1	0

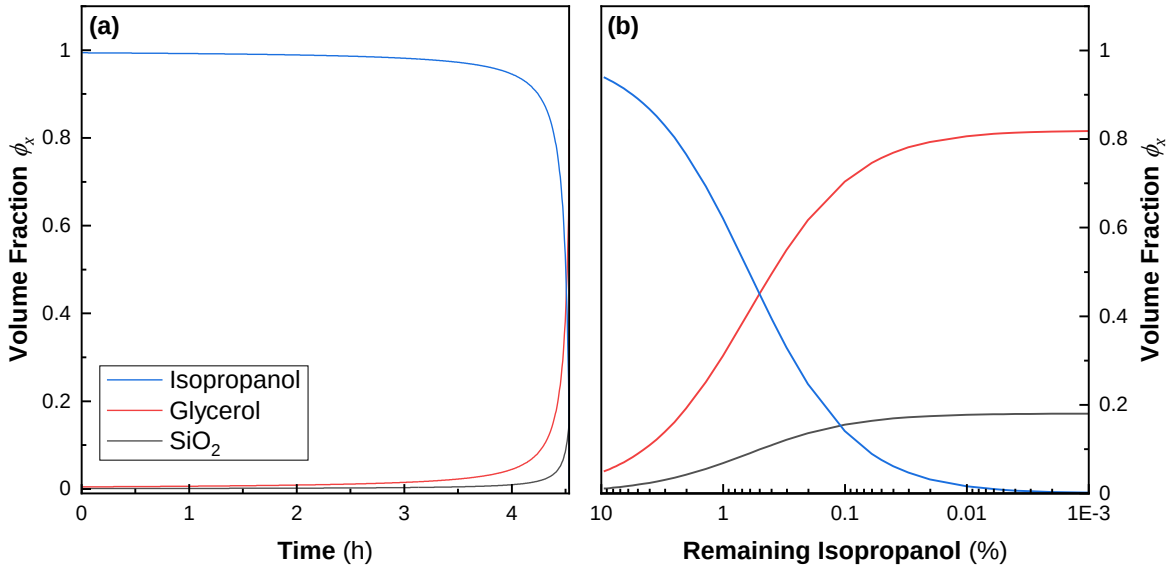

Figure S5. (a) Calculated volume fractions of isopropanol, glycerol and SiO_2 as a function of time during evaporation from a typical 6 mL cuvette used during dip coating. The evaporation rates used to calculate ϕ_x were taken from a fit to the experimentally determined values in (a), the presence of the SiO_2 particles was assumed to not affect evaporation rate and the evaporation of glycerol was considered negligible. (b) The same data expressed as a function of the remaining isopropanol percentage.

Section S7. Rheology of isopropanol – glycerol and isopropanol – glycerol-silica mixtures

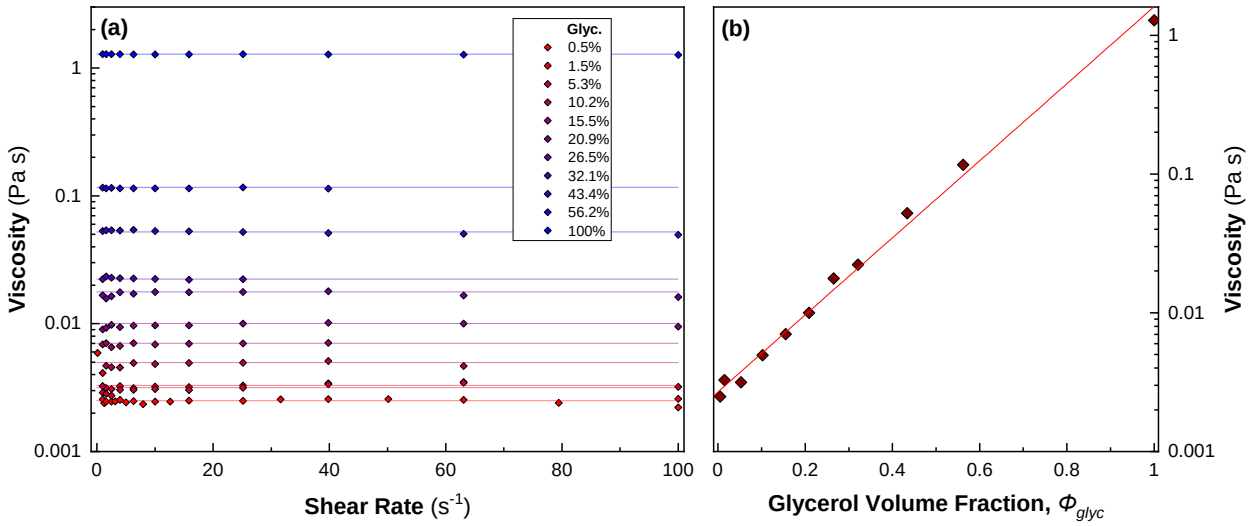

Figure S6. (a) Dynamic viscosity of isopropanol – glycerol mixtures as a function of shear rate in the absence of SiO_2 particles. The glycerol percentages selected correspond to concentrations seen in the solutions in Figure S7.

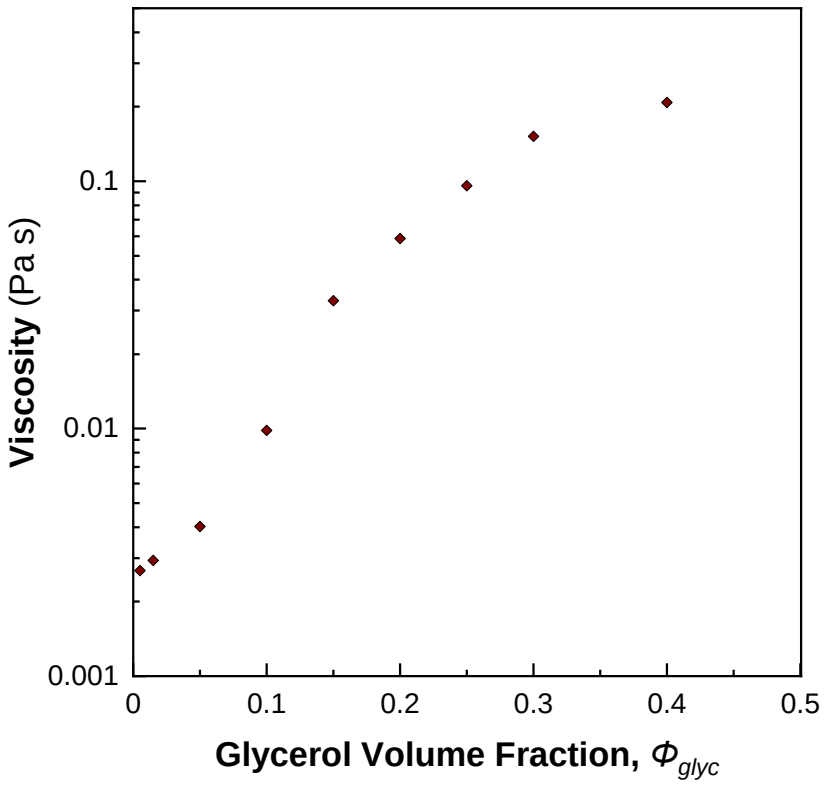

Figure S7. Dynamic viscosity of isopropanol – glycerol – SiO_2 particle mixtures as a function of glycerol volume fraction, ϕ_{glyc}. Because the solutions display shear-thinning, viscosities are given at a single shear rate of 26.83 s^{-1}.

Section S8. Tensiometry of isopropanol – glycerol mixtures

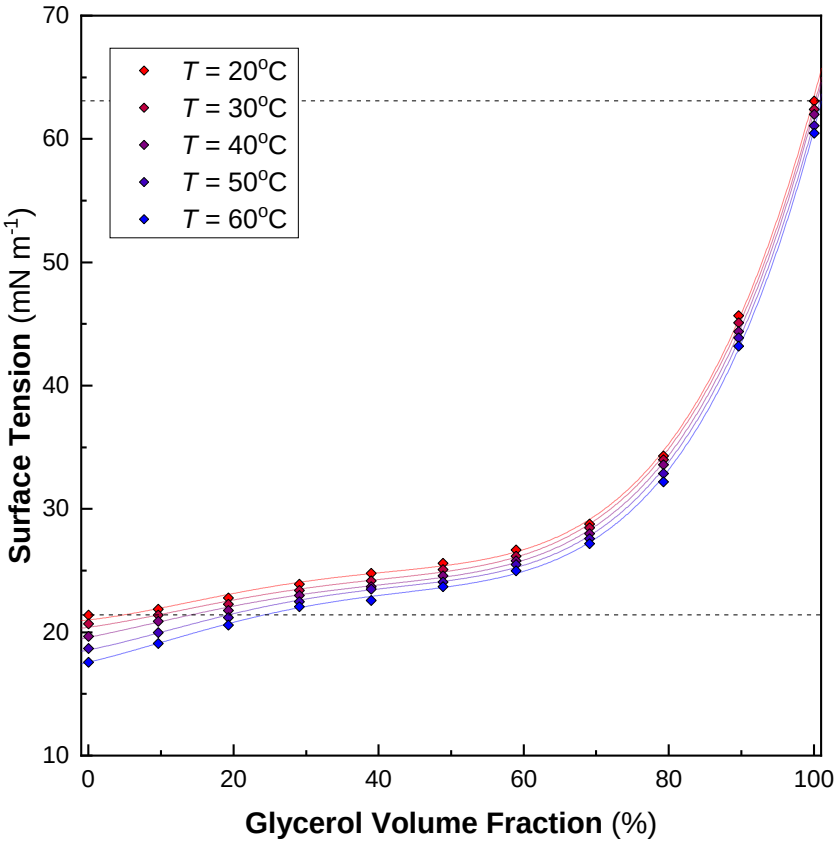

Figure S8. Surface tension of isopropanol-glycerol mixes between 20-60 °C, values taken from the literature.[10]

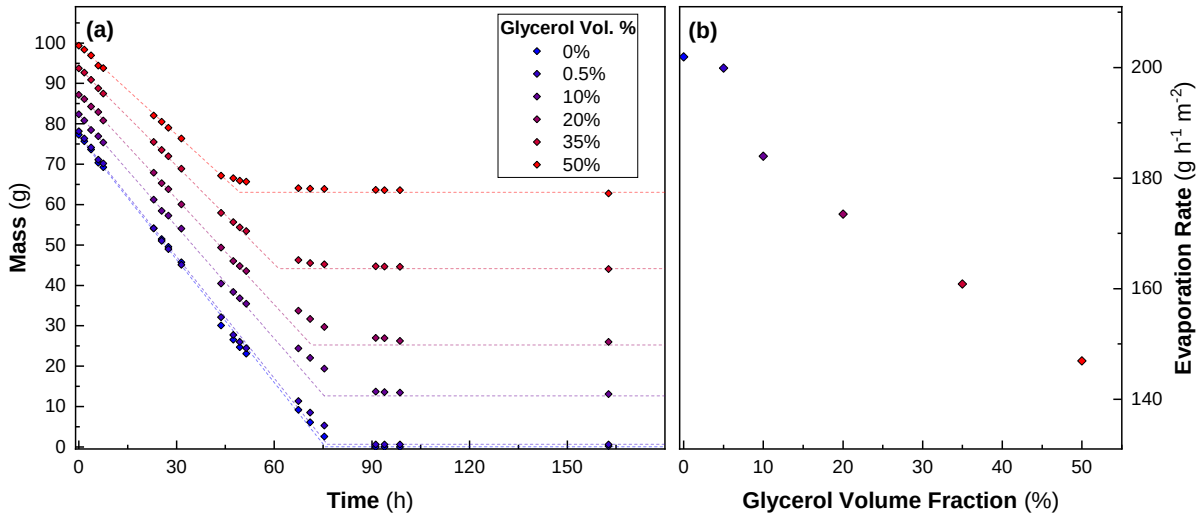

Figure S9. (a) Mass evaporated over time for i-PrOH - glycerol mixtures at 50 °C. (b) Evaporative fluxes as measured from the initial linear section of each mass evaporation curve in (a) as a function of glycerol volume fraction.

Section S9. Patterns of films deposited from a mixture of glycerol and i-PrOH

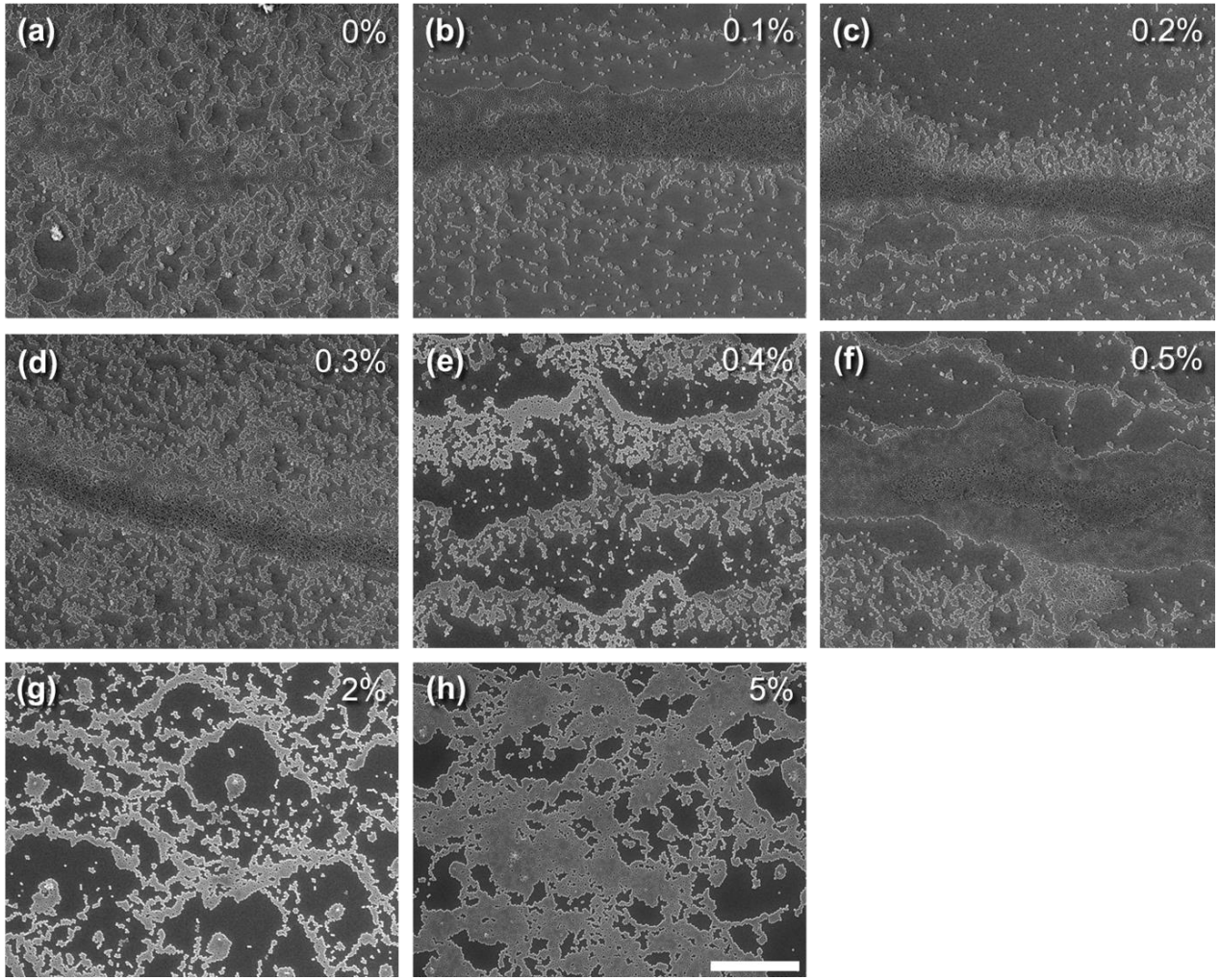

Figure S10. SEM images of dip-coated films prepared at 50 °C, withdrawn at 50 μm s^{-1}, using an initial concentration of 0.11 vol% SiO_2 particles and (a) 0, (b) 0.1 (c) 0.2, (d) 0.3, (e) 0.4, (f) 0.5, (g) 2 and (h) 5 vol% glycerol. All images have the same scale, the scale bar represents 10 μm.

References

(1) Kabir, M. H.; Motin, M. A.; Huque, M. E. Densities and Excess Molar Volumes of Methanol, Ethanol and N-Propanol in Pure Water and in Water + Surf Excel Solutions at Different Temperatures. *Phys. Chem. Liq.* **2004**, *42* (3), 279–290. https://doi.org/10.1080/0031910042000205346.

(2) Bravo-Sánchez, M. G.; Iglesias-Silva, G. A.; Estrada-Baltazar, A.; Hall, K. R. Densities and Viscosities of Binary Mixtures of N-Butanol with 2-Butanol, Isobutanol, and Tert-Butanol from (303.15 to 343.15) K. *J. Chem. Eng. Data* **2010**, *55* (6), 2310–2315. https://doi.org/10.1021/je900722m.

(3) Pang, F.-M.; Seng, C.-E.; Teng, T.-T.; Ibrahim, M. H. Densities and Viscosities of Aqueous Solutions of 1-Propanol and 2-Propanol at Temperatures from 293.15 K to 333.15 K. *J. Mol. Liq.* **2007**, *136* (1), 71–78. https://doi.org/10.1016/j.molliq.2007.01.003.

(4) Ortega, J. Densities and Refractive Indices of Pure Alcohols as a Function of Temperature. *J. Chem. Eng. Data* **1982**, *27* (3), 312–317. https://doi.org/10.1021/je00029a024.

(5) Gliński, J.; Chavepeyer, G.; Platten, J. Surface Properties of Diluted Aqueous Solutions of Tert-butyl Alcohol. *J. Chem. Phys.* **1995**, *102* (5), 2113–2117. https://doi.org/10.1063/1.468733.

(6) Vazquez, G.; Alvarez, E.; Navaza, J. M. Surface Tension of Alcohol Water + Water from 20 to 50 .Degree.C. *J. Chem. Eng. Data* **1995**, *40* (3), 611–614. https://doi.org/10.1021/je00019a016.

(7) Gong, Y.; Shen, C.; Lu, Y.; Meng, H.; Li, C. Viscosity and Density Measurements for Six Binary Mixtures of Water (Methanol or Ethanol) with an Ionic Liquid ([BMIM][DMP] or [EMIM][DMP]) at Atmospheric Pressure in the Temperature Range of (293.15 to 333.15) K. *J. Chem. Eng. Data* **2012**, *57* (1), 33–39. https://doi.org/10.1021/je200600p.

(8) Shirazi, S. G.; Kermanpour, F. Density and Viscosity of 2-Butanol + (1-Propanol, 2-Propanol, or 3-Amino-1-Propanol) Mixtures at Temperatures of (293.15 to 323.15) K: Application of the ERAS Model. *J. Chem. Eng. Data* **2019**, *64* (6), 2292–2302. https://doi.org/10.1021/acs.jced.8b01097.

(9) Gao, J.; Semlali, S.; Hunel, J.; Montero, D.; Battie, Y.; Gonzalez-Rodriguez, D.; Oda, R.; Drisko, G. L.; Pouget, E. Creating Regular Matrices of Aligned Silica Nanohelices: Theory and Realization. *Chem Mater* **2020**, *32* (2), 821. https://doi.org/10.1021/acs.chemmater.9b04372.

(10) Erfani, A.; Khosharay, S.; Aichele, C. P. Surface Tension and Interfacial Compositions of Binary Glycerol/Alcohol Mixtures. *J Chem Thermodyn* **2019**, *135*, 241. https://doi.org/10.1016/j.jct.2019.03.014.